Journal of Rock Mechanics and Geotechnical Engineering xxx (xxxx) xxx

Contents lists available at ScienceDirect

Journal of Rock Mechanics and Geotechnical Engineering

journal homepage: www.jrmge.cn

Full Length Article

Effects of data smoothing and recurrent neural network (RNN) algorithms for real-time forecasting of tunnel boring machine (TBM) performance

Feng Shan, Xuzhen He, Danial Jahed Armaghani, Daichao Sheng*

School of Civil and Environmental Engineering, University of Technology Sydney, NSW, 2007, Australia

A R T I C L E I N F O

Article history:
Received 7 March 2023
Received in revised form
5 May 2023
Accepted 15 June 2023
Available online xxx

Keywords:
Tunnel boring machine (TBM)
Penetration rate (PR)
Time series forecasting
Recurrent neural network (RNN)

A B S T R A C T

Tunnel boring machines (TBMs) have been widely utilised in tunnel construction due to their high efficiency and reliability. Accurately predicting TBM performance can improve project time management, cost control, and risk management. This study aims to use deep learning to develop real-time models for predicting the penetration rate (*PR*). The models are built using data from the Changsha metro project, and their performances are evaluated using unseen data from the Zhengzhou Metro project. In one-step forecast, the predicted penetration rate follows the trend of the measured penetration rate in both training and testing. The autoregressive integrated moving average (ARIMA) model is compared with the recurrent neural network (RNN) model. The results show that univariate models, which only consider historical penetration rate itself, perform better than multivariate models that take into account multiple geological and operational parameters (GEO and OP). Next, an RNN variant combining time series of penetration rate with the last-step geological and operational parameters is developed, and it performs better than other models. A sensitivity analysis shows that the penetration rate is the most important parameter, while other parameters have a smaller impact on time series forecasting. It is also found that smoothed data are easier to predict with high accuracy. Nevertheless, over-simplified data can lose real characteristics in time series. In conclusion, the RNN variant can accurately predict the next-step penetration rate, and data smoothing is crucial in time series forecasting. This study provides practical guidance for TBM performance forecasting in practical engineering.

1. Introduction

Mechanised tunnelling is widely used in underground projects, e.g. subways, railways, water conveyance systems, gas transmission pipelines, underground mines. Tunnel boring machines (TBMs), including earth pressure balance shields, refer to as machines for excavating tunnels with a circular full-face cutterhead equipped with disc cutters. TBMs have many advantages over conventional drill-and-blast method, including higher efficiency, safer workplaces, minimal environmental disturbance, and reduced project costs (Rostami, 1997). The continuous cutting, mucking, and lining installation processes of TBM tunnelling greatly increases efficiency compared to conventional methods. However, tunnel collapse, rockburst, water inrush, and machine jamming remain major challenges in complex geotechnical conditions. The penetration rate (PR), an indicator of TBM performance, is calculated as the boring distance divided by the working time and is crucial for project time management and cost control. Forecasting the penetration rate ahead of a cutterhead in real time can also help onsite engineers to adjust TBM operational parameters promptly. The prediction of TBM penetration rate is challenging as it depends on various factors, including geological and operational parameters (GEO and OP) and machine specifications.

Over the years, many researchers have proposed various theoretical and empirical methods to study the relationship between TBM performance and other related parameters. Ozdemir (1977), Rostami et al. (1996), Yagiz (2002) and Hassanpour et al. (2010) developed theoretical methods to provide a fundamental understanding of the mechanics of TBM cutting. Nevertheless, they have limitations in accurately representing real rock mass conditions in field. On the other hand, empirical methods are generally proposed based on field performance and rock properties (Rostami et al., 1996; Bruland, 1998; Barton, 1999; Sapigni et al., 2002; Yagiz,

* Corresponding author.
E-mail address: daichao.sheng@uts.edu.au (D. Sheng).
Peer review under responsibility of Institute of Rock and Soil Mechanics, Chinese Academy of Sciences.

https://doi.org/10.1016/j.jrmge.2023.06.015
1674-7755

2008; Hassanpour et al., 2010; Rostami, 2016). Empirical methods study regressive correlations between various parameters, e.g. uniaxial compressive strength, Brazilian tensile strength, rock quality designation, rock mass rating, thrust force (TH), cutterhead torque (TO), revolutions per minute (RPM). It is challenging to develop sophisticated empirical equations that consider several simulation parameters, particularly considering uncertain factors. The accuracy of theoretical and empirical methods is acceptable but not high. Therefore, they have been useful in scheduling TBM projects before the start of construction.

Machine learning techniques are highly effective and versatile in capturing complex, nonlinear relationships, and have been successfully applied to TBM tunnelling, e.g. surface settlement (Zhang et al., 2020a, 2021a; Kannangara et al., 2022), rock mass classification (Sousa and Einstein, 2012; Wu et al., 2021; Hou et al., 2022), and others (Hasanpour et al., 2020; Liu et al., 2021). Researchers attempted to predict TBM performance using machine learning algorithms, e.g. artificial neural network, fuzzy logic, support vector regression, random forest, adaptive neuro-fuzzy inference system, and classification and regression tree (Grima et al., 2000; Benardos and Kaliampakos, 2004; Mahdevari et al., 2014; Salimi et al., 2016; Sun et al., 2018; Bardhan et al., 2021; Parsajoo et al., 2021). As various hyperparameters result in diverse models, optimisation technologies are employed to find a near-optimal model. Particle swarm optimisation, Bayesian optimisation, and grey wolf optimiser are used to predict TBM performance (Yagiz and Karahan, 2011, 2015; Armaghani et al., 2017, 2019; Zhang et al., 2020b; Lin et al., 2022a; Yang et al., 2022; Lin et al. (2021), Huang et al. (2022), and Lin et al., 2022a, b) began incorporating both current and historical values to predict TBM performance, which is essentially a regression analysis than time series forecasting. These models are generally more accurate, and are considered black boxes between TBM performance and related parameters. They are highly flexible in adding or filtering related parameters and implicitly capturing the impact of uncertain parameters. However, they are limited in their applicability, as they are specific to one or a few similar tunnel projects, and cannot be generalised to different types of TBMs and geological conditions (Zhang et al., 2021b). Another obstacle to TBM tunnelling research is the challenge of data sharing due to commercial confidentiality. Additionally, TBM performance belongs to operational parameters that are collected in real time by the TBM acquisition system and cannot be obtained prior to the start of a project. TBM performance models by Armaghani et al. (2017), Sun et al. (2018), Lin et al. (2021) and Yang et al. (2022) are not feasible to apply in practice because the inputs of operational parameters are still unknown. Data from completed tunnel projects can only be utilised for the training of models in practical applications.

As TBM performance is determined by current inputs without the help of historical values, the aforementioned models are not ideal for real-time prediction (Gao et al., 2019; Xu et al., 2021). A more feasible and preferred outcome for TBM operation is the capacity of forecasting future values using both current and historical data, also known as time series forecasting (Bontempi et al., 2012; Pavlyshenko, 2019). Time series forecasting of TBM performance is a real-time prediction to predict unknown TBM performance in the future. This real-time prediction is not intended for overall project time management, but rather for a short-term forecast ahead of the cutterhead. It is crucial to make necessary adjustments when potential issues are detected based on predicted TBM performance ahead of the cutterhead.

High-frequency data are collected directly from the data acquisition system every few seconds or minutes. Predicting next-step TBM performance in high frequency can be achieved with high accuracy, and recurrent neural networks (RNNs) and long short-term memory, which incorporate current and historical inputs, have been shown to perform better than other machine learning algorithms (Gao et al., 2019; Qin et al., 2021; Shi et al., 2021; Wang et al., 2021). However, it is less meaningful to know TBM performance just a few seconds or centimetres in advance. Subsequently, multi-step forecasts were explored, and it was found that errors increase significantly with increasing forecast horizon (Shi et al., 2021). Erharter and Marcher (2021) were unable to make a long-term forecast of cutterhead torque beyond the next 100 steps, corresponding to a distance of 5.5 m ahead of the cutterhead.

High-frequency data can be preprocessed into low-frequency data where each data point represents a fixed segment or working cycle, typically spanning 1–2 m. For example, the Yingsong Water Diversion Project is a low-frequency dataset divided into working cycles, including start-up, ascending, steady-state, and end stages. Li et al. (2021) and Xu et al. (2021) used the time series from the first 2-min ascending stage to forecast the average operational parameters at the steady-state stage. Feng et al. (2021) developed three models to predict next-step TBM performance in similar geological conditions for diorite, granite, and limestone. The prediction involved averaging data points corresponding to one working cycle or tunnel segment, providing ample time for engineers to make adjustments between two data points. Shan et al. (2022) successfully trained time series forecasting models on the dataset from Changsha metro and evaluated the models on the dataset from Zhengzhou metro, which had different geological conditions. However, as the models predicted further into the future, the accuracy decreased due to the reduced impact of parameters farther away from the TBM cutterhead on TBM performance (Shan et al., 2022, 2023).

Forecasting TBM performance has generated much anticipation but with little success to date. Fig. 1 is a technical roadmap for time series forecasting of TBM performance. On the one hand, high-frequency forecasts rely solely on historical TBM performance (Erharter and Marcher, 2021; Shi et al., 2021) or historical TBM performance and operational parameters (Gao et al., 2019; Qin et al., 2021; Wang et al., 2021). Such forecasts overlook geological conditions ahead of the cutterhead and have limited success in predicting TBM performance a few seconds or centimetres ahead. On the other hand, low-frequency forecasts can predict a few metres in advance but have a limited number of samples after preprocessing (Shan et al., 2022), which in turn affects the model robustness. As tunnelling data become more accessible, it may be possible to interrogate TBM specification, e.g. TBM type, TBM diameter, and the number of cutters.

This study aims to build models using low-frequency data to predict next-step penetration rate, while considering current and historical penetration rates and other geological and operational parameters. Two datasets with different geological conditions are used to examine the generalisability of the models. Most importantly, this study also conducts sensitivity analysis and investigates the effects of data smoothing.

2. Methodology

2.1. data smoothing technique

Smoothing is a technique used to eliminate the fine-grained variation in time series to remove noise and better expose the signal of underlying information. A moving average can be used to create a smoothed version, where values are obtained by taking the average of observations in the original time series. Note that a moving average can also be used to predict future values. Nevertheless, model performance is unsatisfied, as it fails to account for complex relationships and respond adequately to rapid changes.

Please cite this article as: Shan F et al., Effects of data smoothing and recurrent neural network (RNN) algorithms for real-time forecasting of tunnel boring machine (TBM) performance, Journal of Rock Mechanics and Geotechnical Engineering, https://doi.org/10.1016/j.jrmge.2023.06.015

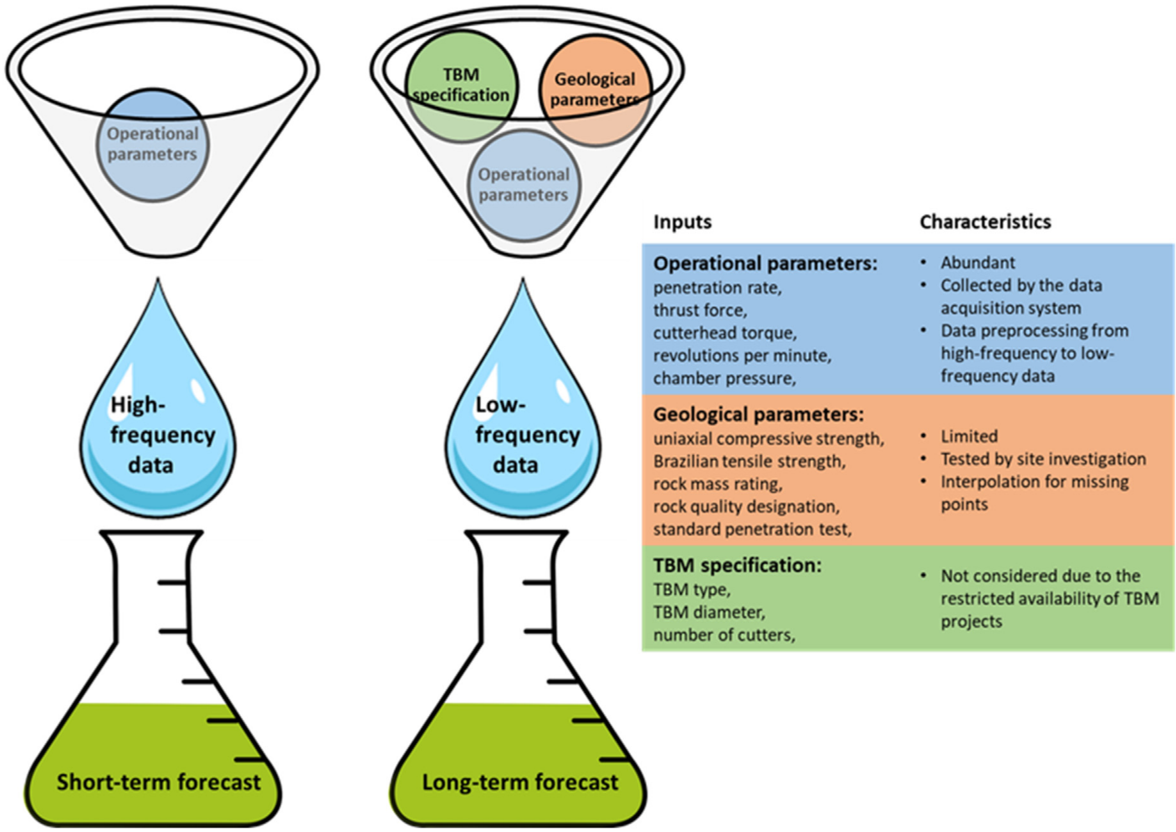

Fig. 1. Technical roadmap for time series forecasting of TBM performance.

There are two main types of moving average methods, i.e. simple moving average (SMA) and exponential moving average (EMA). EMA places greater weight and significance on the most recent data points (Roberts, 2000) than SMA, which applies an equal weight to all observations within the period. These moving averages can be expressed as

$$s_t = (x_t + x_{t-1} + \ldots + x_{t-k+1}) / k \tag{1}$$

$$s_t = \alpha x_t + (1-\alpha) s_{t-1} \tag{2}$$

where s_t is the smoothed datum, x_t is the original datum, t is time, k is sliding window size, α is the smoothing factor between 0 and 1.

In Eq. (1), the SMA is the unweighted mean of the past k data points. In Eq. (2), the EMA is determined by a smoothing factor α. The smoothed statistic s_t is a weighted average of the recent observation x_t and the previous smoothed statistic s_{t-1}. Values of α closer to 1 correspond to less smoothing and are more sensitive to recent changes in the data. Conversely, values of α closer to 0 correspond to a higher degree of smoothing and are less responsive to recent changes.

2.2. Autoregressive integrated moving average (ARIMA)

An ARIMA model is a widely used statistical method to predict future values based on historical values (Box and Pierce, 1970). The ARIMA model is characterised by three parameters: p for the number of autoregressive lags, d for the degree of differencing, and q for the size of moving average window. It is formulated in Eq. (3) as

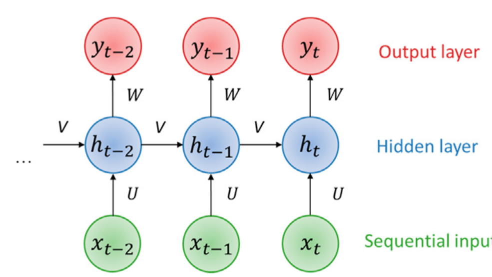

Fig. 2. Schematic diagram of RNN architecture.

$$x_t = \mu + \epsilon_t + \sum_{i=1}^{p} \varphi_i x_{t-i} + \sum_{i=1}^{q} \theta_i \epsilon_{t-i} \tag{3}$$

where x_t, ϵ_t are the output and error at time t, and μ is the mean value of the time series. Autoregression involves a sigma summation of p terms, where each term is the product of coefficients φ_i and outputs of the respective lags x_{t-i}. Moving average involves a sigma summation of q terms, where each term is the product of coefficients θ_i and errors of the respective time ϵ_{t-i}. An important requirement for an ARIMA model is that the time series is stationary and not depend on time. Differencing is a common technique used to transform a non-stationary series into a stationary one, which can remove trend and seasonal structures but does not address non-stationary in the variance or autocovariance.

Please cite this article as: Shan F et al., Effects of data smoothing and recurrent neural network (RNN) algorithms for real-time forecasting of tunnel boring machine (TBM) performance, Journal of Rock Mechanics and Geotechnical Engineering, https://doi.org/10.1016/j.jrmge.2023.06.015

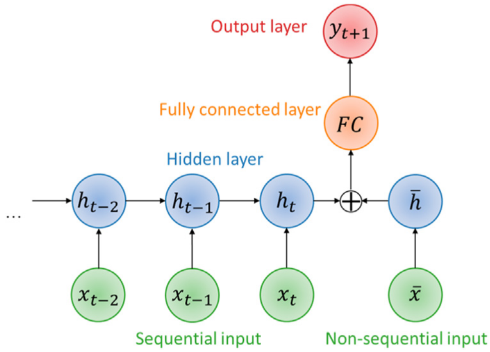

Fig. 3. Schematic diagram of the RNN variant.

2.3. Recurrent neural network (RNN)

The RNN is a leading algorithm that employs an internal state to solve sequential data problems, e.g. speech recognition, language translation, or time series forecasting (Schuster and Paliwal, 1997; Graves et al., 2013). The RNN architecture is illustrated in Fig. 2, transferring information from former neurons to latter ones. For example, the last hidden state h_{t-1} and recent inputs x_t contribute to the recent hidden state h_t in Eq. (4). The recent output y_t extracts temporal features from h_t in a linear transformation in Eq. (5).

$$h_t = \tanh(Ux_t + Vh_{t-1} + b_h) \tag{4}$$

$$o_t = Wh_t + b_o \tag{5}$$

where U, V, W are the shared weights, and b_h and b_o are the shared biases across the sequence.

To determine the importance of the input to the network, activation functions are applied, e.g. sigmoid, ReLU, and tanh functions. In RNN, the tanh(x) function returns the hyperbolic tangent of the input. RNN can be prone to the issue of vanishing or exploding gradients when the input sequences are too long (Bengio et al., 1994). This issue is not apparent in this study as the length of input sequences is limited to only 20 data points.

2.4. An RNN variant

In addition to the time series data, there are parameters that are not time-dependent but have an impact on future values. These inputs can be categorized into two types: sequential and non-sequential. While RNN is adept at handling sequential data owing to its loop architecture, it cannot process non-sequential data. Therefore, we propose a modified version of RNN with a fully connected layer for non-sequential data, as shown in Fig. 3.

The inherent of algorithms is to extract relevant features from input data. RNN extracts temporal features from the time series x_{t-2}, x_{t-1} and x_t through Eq. (4) with a result of the recent hidden state h_t. Non-sequential inputs $\bar{x}_t$ are fully connected to extract hidden features $\bar{h}_t$ followed by a ReLU function. After feature extraction, h_t and $\bar{h}_t$ are obtained, each with a length corresponding to their respective hidden size. A fully connected layer FC is concatenated by copying the elements of two hidden arrays, with a total length of h_t and $\bar{h}_t$. Finally, y_{t+1} is fully connected with FC as a final output layer. By leveraging both sequential and non-sequential inputs, the proposed method deeply exploited and utilised the available information to predict future values.

2.5. Sensitivity analysis

A model can be decomposed using Eq. (6), and the variance of the output $Var(y)$ can be decomposed using Eq. (7) under orthogonality constraints (Hoeffding, 1992). To analyse how much the variance of each parameter affects the output variance, Sobol (1990) introduced the variance-based sensitivity analysis, also known as the Sobol method. The direct effect of each parameter is measured by the first-order Sobol index S_i in Eq. (8). The total-effect Sobol index S_{Ti} takes into account the sensitivity of first-order effect and the sensitivity due to interactions between a given parameter and all other parameters in Eq. (9). If a parameter has a low Sobol index, then variations in the parameter lead to comparatively small variations in the model output, and vice versa.

$$y = f_0 + \sum\nolimits_{i=1}^{p} f_i(x_i) + \sum\nolimits_{i<j}^{p} f_{ij}(x_i, x_j) + \cdots + f_{1,2,\cdots,p}(x_1, x_2, \ldots, x_p) \tag{6}$$

$$Var(y) = \sum\nolimits_{i=1}^{p} V_i + \sum\nolimits_{i<j}^{p} V_{ij} + \cdots + V_{1,2,\cdots,p} \tag{7}$$

$$S_i = \frac{V_i}{Var(y)} \tag{8}$$

$$S_{Ti} = 1 - \frac{Var_{x_{\sim i}}[E_{x_i}(y|x_{\sim i})]}{Var(y)} \tag{9}$$

where f_0 is a constant, f_i is a function of x_i, f_{ij} is a function of x_i and x_j, $V_i = Var_{x_i}[E_{x_{\sim i}}(y|x_i)]$ and $V_{ij} = Var_{x_{ij}}[E_{x_{\sim ij}}(y|x_i, x_j)] - V_i - V_j$ are the expanded forms of the expected value, and $x_{\sim i}$ indicates all parameters except x_i.

3. Case study

3.1. Project preview

Changsha metro line 4, a rapid transit line located in Changsha, China, was excavated and opened for use in May 2019. The line spans approximately 33.5 km in the northwest-southeast direction, between Guanziling and Dujiaping. Five sections between six stations were investigated in this study: Liugoulong, Wangyuehu, Yingwanzhen, Hunan Normal University, Hunan University, and Fubuhe. The tunnel was excavated using an earth pressure balance shield with a cutterhead diameter and length of 6.28 m and 8.735 m, respectively. The cutterhead has an open ratio of 35%. To provide structural support, segmental lining was used to form a tube along the tunnel alignment. The segments were prefabricated in manufacturing plants with a width of 1.5 m and outer and inner diameters of 6 m and 5.4 m, respectively. Operational parameters were recorded by the data acquisition system at 1-min intervals. Geological conditions along the five sections were obtained by site investigation and experiments. The machine excavated the tunnel in rocks, e.g. slate, limestone, mudstone, and sandstone, and in soils, e.g. silty clay, gravel, and marlite (Zhang et al., 2019, 2021c). Fig. 4 shows the geographical location and typical geological profile of Changsha metro.

Zhengzhou metro line 3 is a rapid transit line that runs from northwest to southeast in Zhengzhou, China, covering a total length of 24.5 km and 23 stations. The tunnel project was completed by earth pressure balance shields from December 2016 to December 2020. We investigated a section between Jinshuilu and Taikanglu

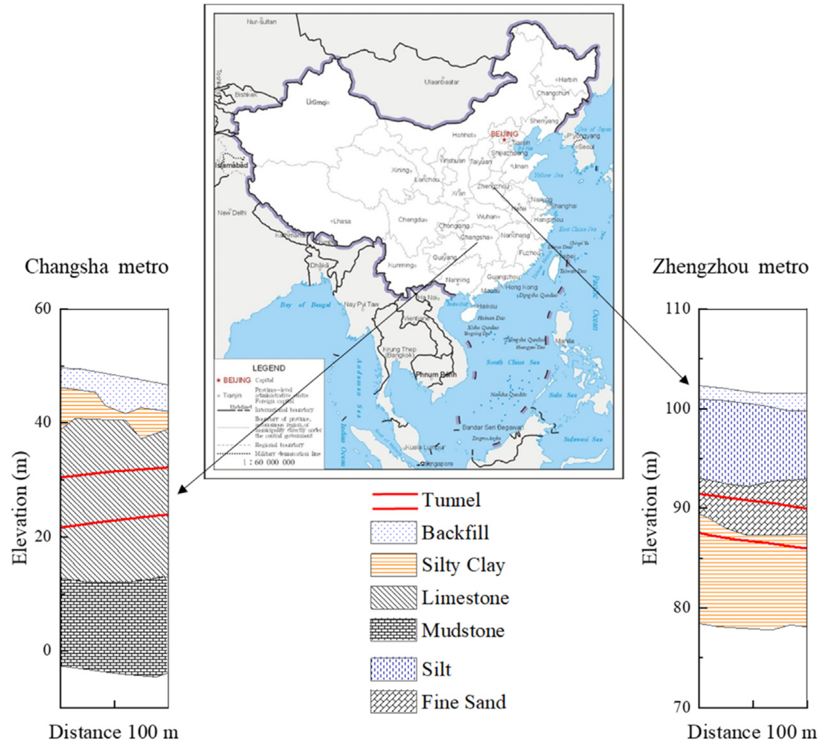

Fig. 4. Geographical locations and typical geological profiles of Changsha and Zhengzhou metros.

stations. The segment width in Zhengzhou is the same as that in Changsha, but the outer and inner diameters are 3.1 m and 2.75 m, respectively. Unlike the geological conditions of the Changsha section, the Zhengzhou section was excavated in soil strata consisting of fine sand and silty clay, with top layers of backfills and silt in Fig. 4 (Zhang et al., 2020a).

3.2. Statistical analysis

Operational parameters are collected every minute by the data acquisition system at high frequency, while geological parameters are measured per segment at low frequency. Zhang et al. (2020a) preprocessed the operational data to match the geological data in five steps.

(1) Removal of empty data due to TBM maintenance, cutters change, breakdowns, or tunnel collapses;
(2) Removal of the first and last 2.5% of operational data at one segment;
(3) Detection and deletion of outliers based on the Mahalanobis distance;
(4) Utilising wavelet transform to eliminate noise in time series data; and
(5) Averaging operational data at one segment as one sample.

Penetration rate (PR), thrust force (TH), cutterhead torque (TO), face pressure (FP), and revolutions per minute (RPM) are the operational parameters, reflecting TBM performance in tunnel construction. Concerning geological parameters, cover depth (CD) is the depth over the tunnel crown, water table (WT) is tunnel depth below the water table, ground condition (GC) at the tunnel face can be classified into four types, i.e. soil, gravel, rock and mixed-face ground, which are marked as 1, 2, 3 and 4, respectively. Modified standard penetration test (mSPT) is expressed by

Table 1
Statistical details of geological and operational parameters.

Parameter	Symbol	Unit	Minimum	Maximum	Average value
Penetration rate	*PR*	m/h	0.24	4.56	2.1
Thrust force	*TH*	MN	4.08	23.8	11.56
Cutterhead torque	*TO*	MN m	0.63	4.82	2.53
Face pressure	*FP*	100 kPa	0	2.1	0.95
Revolutions per minute	*RPM*	rev/min	0.46	2.16	1.41
Cover depth	*CD*	m	9.09	31.65	17.86
Water table	*WT*	m	0	25.11	8.7
Ground condition	*GC*	–	1	4	2.69
Modified standard penetration test	*mSPT*	–	0	39.92	6.03

$$N'_{63.5} = \sum_{i=1}^{n} \frac{t_i}{h} \frac{h_i}{h} N_{63.5} \tag{10}$$

where $N'_{63.5}$ is the modified standard penetration test, $N_{63.5}$ is the blow count of standard penetration test, h is the cover depth over the tunnel crown, t_i is the thickness of each layer, and h_i is the cover depth of each layer. The basic statistical details of these parameters are presented in Table 1.

In Fig. 5, the time series of geological and operational parameters along the tunnel alignment is displayed, with blue lines presenting data from Changsha metro and orange lines presenting data from Zhengzhou metro. The horizontal coordinate includes a total of 550 time series data points, with each data point representing a segment of length 1.5 m. It was assumed that the two datasets are equally spaced in the sequence, despite samples being removed or missing. *GC* from Changsha is mainly of rock at the tunnel face with a value of 3, while that from Zhengzhou is soil with a value of 1. It is observed that mSPT is quite different between

Please cite this article as: Shan F et al., Effects of data smoothing and recurrent neural network (RNN) algorithms for real-time forecasting of tunnel boring machine (TBM) performance, Journal of Rock Mechanics and Geotechnical Engineering, https://doi.org/10.1016/j.jrmge.2023.06.015

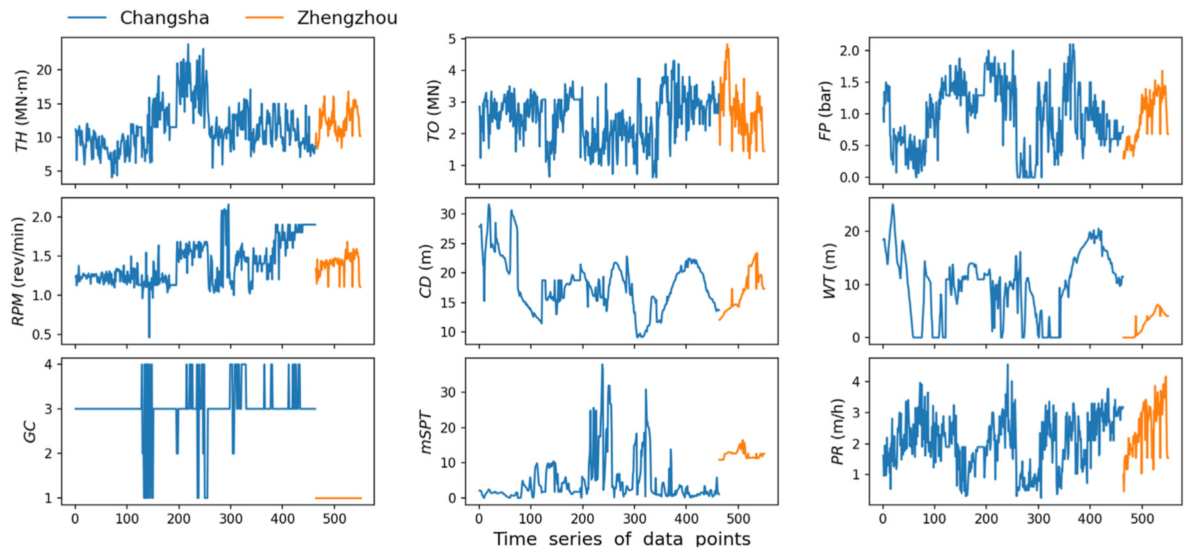

Fig. 5. Time series of geological and operational parameters from Changsha and Zhengzhou metros.

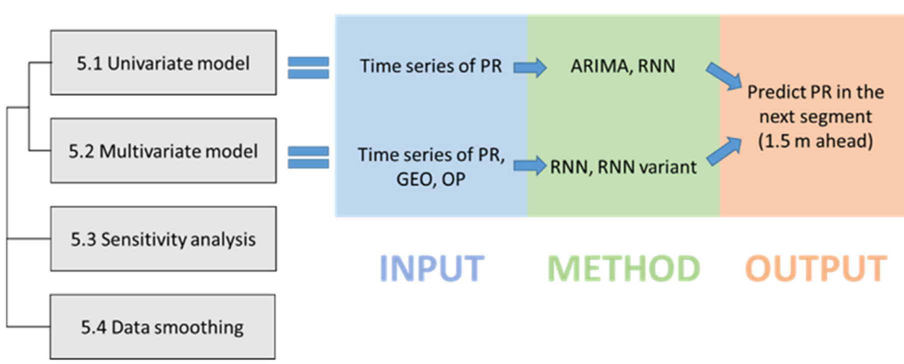

Fig. 6. Framework for one-step forecasts of penetration rate.

Changsha and Zhengzhou. Therefore, it is challenging to check the generalisability that a trained model based on data from Changsha adapts properly to unseen data from Zhengzhou.

3.3. Step-by-step procedure

In this study, a framework for one-step forecast is presented in Fig. 6, categorising input parameters into PR, geological parameters, and operational parameters. The focus of the study is on one-step PR forecast, where univariate models use historical PR value to predict PR value in the next segment, while multivariate models combine historical PR, GEO, and OP. A sensitivity analysis is conducted to study the impacts of input parameters on future penetration rate. Additionally, the study examines the effects of data smoothing and discusses the dilemma of balancing noise reduction and real data preservation in the original time series.

4. Forecasting modelling

4.1. Data processing

Fig. 7 depicts a modelling flowchart consisting of three phases, i.e. data processing, training, and evaluation. Noise can affect the intrinsic characteristics of a time series, introduced by sensor errors or document digitalisation. Shan et al. (2022) used SMA to remove noise by applying an equal weight to the past five data points. In this study, EMA is applied to creating smoothed data, which places a greater weight and significance on the most recent data points. Fig. 8a illustrates the original data in blue and the smoothed data with a smoothing factor of 0.67 in orange. A strong correlation of 0.9456 exists between them, and sharp changes in the time series are especially smooth. The residuals between the original and smoothed penetration rate are normally distributed with a mean near 0 and a standard deviation of 0.2068 in Fig. 8b. The effects of data smoothing will be discussed later in Section 5.4.

The parameters are scaled to a standard, dimensionless scale because they have different units and magnitudes. Min-max normalisation performs a linear transformation in Eq. (11), scaling the data between 0 and 1. Normalisation can help stabilise the gradient descent for faster model convergence. However, while inputs are normalised, outputs are not. Finally, the normalised inputs and outputs are configured sequentially into different array shapes corresponding to different methods.

$$x_{nor} = \frac{x - x_{min}}{x_{max} - x_{min}} \quad (11)$$

where x and x_{nor} are the original and scaled data; and x_{max} and x_{min} correspond to the maximum and minimum in the data, respectively.

Please cite this article as: Shan F et al., Effects of data smoothing and recurrent neural network (RNN) algorithms for real-time forecasting of tunnel boring machine (TBM) performance, Journal of Rock Mechanics and Geotechnical Engineering, https://doi.org/10.1016/j.jrmge.2023.06.015

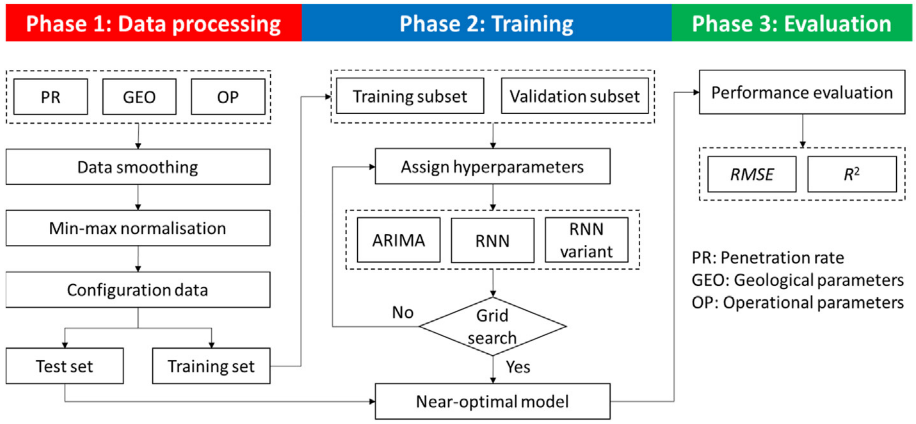

Fig. 7. Flowchart of developing time series forecasting models by deep learning.

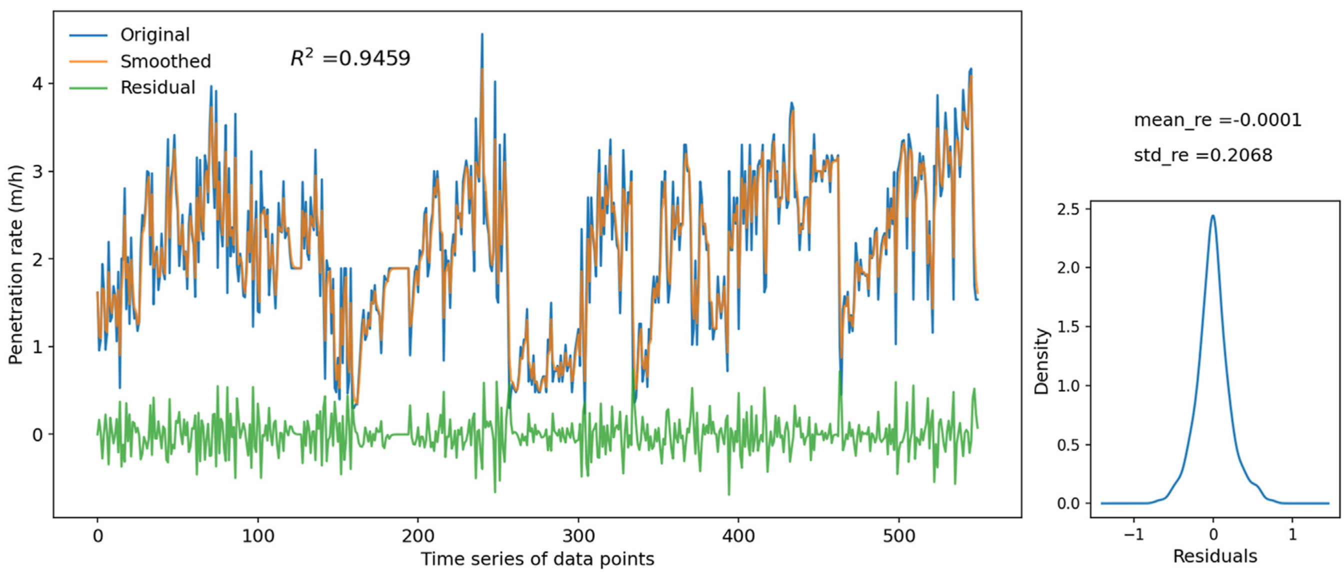

Fig. 8. Time series of (a) original, smoothed penetration rate, and residuals and (b) kernel density estimation of residuals.

4.2. Training

During the training process, the data from Changsha are randomly split into training and validation subsets, with a percentage of 80% and 20%, respectively. Hyperparameters, e.g. hidden size, learning rate, and batch size, can affect model performance but are not trained in the learning process. We initialise or assign hyperparameters and then use different methods to build a model based on training and validation data. An Adam optimiser is used to iteratively update weights and biases until the loss function of the mean squared error converges. To reduce computation cost and prevent possible over-fitting, early stopping is applied, which stops the learning process when validation loss does not decrease over a given number of epochs.

At this point, the learning process has resulted in a converged model with assigned hyperparameters, rather than a near-optimal model. Hyperparameter tuning is then applied to identifying the best combination of hyperparameters by calculating the lowest validation loss. To accomplish this, a grid search exhaustively searches through the hyperparameter space, updating hyperparameters and replacing the near-optimal model at the same time. Besides, Bayesian optimisation can be applied to geotechnical problems (Zhang et al., 2021d, 2022a), which enables to balance exploration and exploitation to converge to the optimum of machine learning models quickly.

4.3. Evaluation

Overfitting occurs when a model perfectly fits its training data (i.e. extremely good model performance in training). Nevertheless, its performance is poor when evaluated with unseen data (i.e. low model performance in testing). As a result, the model performance in testing is an indicator of the quality of the trained model. The near-optimal model is evaluated using the test data from Zhengzhou, where evaluation metrics include the root mean squared error ($RMSE$) and coefficient of determination (R^2) defined as

$$RMSE = \sqrt{\frac{1}{n}\sum_{i=1}^{n}(y_i - \widehat{y}_i)^2} \tag{12}$$

$$R^2 = 1 - \frac{\sum_{i=1}^{n}(y_i - \widehat{y}_i)^2}{\sum_{i=1}^{n}(y_i - \overline{y})^2} \tag{13}$$

where y_i and $\hat{y}_i$ are the measured and predicted values, and $\bar{y}$ is the mean of measured value. *RMSE* represents the difference between the measured and predicted values, and has the same magnitude as targets. R^2 is a performance metric between 0 and 1, where a larger value indicates a higher accuracy between predicted and measured values, and vice versa.

5. Results and discussion

The focus of this study is to predict the next penetration rate (1.5 m ahead) using historical data. Time series forecasting models are trained by the dataset from Changsha metro, and their model performance is evaluated by *RMSE* and R^2 on the dataset from Zhengzhou metro, as summarised in Table 2. The hyperparameters for the near-optimal models are presented in Table 3. In the table, $\{PR_t\}$ refers to as time series data up to recent penetration rate, and PR_{t+1} represents penetration rate in the next step. Hidden size 1 refers to the hidden size derived from time series data of penetration rate, while hidden size 2 refers to the hidden size derived from the last step of geological and operational parameters in the RNN variant model.

5.1. Univariate models

5.1.1. ARIMA

In statistics, Model #1 uses historical penetration rates to predict the next-step penetration rate (0–1.5 m) by ARIMA. The parameters of p, d, and q are autoregression, differencing, and moving average, which are determined with the help of an auto-ARIMA package from the Pmdarima library in Python. On this basis, a near-optimal ARIMA model is built with $p = 1$, $d = 1$, $q = 1$, and the equation can be expressed as $DIFF(PR_t) = \mu + \epsilon_t + \varphi DIFF(PR_{t-1}) + \theta\epsilon_{t-1}$, where $DIFF(PR)$ is the first difference in penetration rate. Fig. 9 shows the training and test results, where the predicted values closely follow the trend of the measured values. The statistical ARIMA model is evaluated with *RMSE* of 0.4176 and R^2 of 0.6864.

5.1.2. RNN

In Model # 2, the best combination of hyperparameters consists of a window size of 3, a hidden size of 20, a learning rate of 0.005, a number of layers of 1, and a batch size of 32. In Fig. 10, both training and validation losses decrease dramatically at the beginning and then slightly decrease after the epoch of 10. The embedded Fig. 10 provides a detailed view of the changes in the loss function between epochs 4 and 14. To prevent overfitting, the early stopping saves a converged model at the epoch of 62, which yields the minimum validation loss. During the last 20 epochs (62–82), the validation loss no longer decreases, showing that the saved model is subjected to validation data without overfitting.

Table 2
Model performance for time series forecasting of penetration rate.

Model	Smoothing factor	Method	Input	Output	*RMSE*	R^2
#1	0.67	ARIMA	$\{PR_t\}$	PR_{t+1}	0.4176	0.6864
#2	0.67	RNN	$\{PR_t\}$		0.4034	0.6741
#3	0.67	RNN	$\{PR_t\}, \{GEO_t\}$		0.4046	0.6718
#4	0.67	RNN	$\{PR_t\}, \{OP_t\}$		0.4117	0.6593
#5	0.67	RNN	$\{PR_t\}, \{GEO_t\}, \{OP_t\}$		0.4053	0.6638
#6	0.67	RNN variant	$\{PR_t\}, GEO_t, OP_t$		0.3952	0.6913
#7	1	RNN	$\{PR_t\}$		0.6164	0.4061
#8	0.5	RNN			0.3092	0.7916
#9	0.33	RNN			0.2026	0.9004
#10	0.2	RNN			0.1239	0.9610

Table 3
Hyperparameters in the near-optimal models.

ARIMA model	Autoregression	Moving average	Differencing			
#1	1	1	1			
RNN model	Batch size	Time step	Hidden size 1	Hidden size 2	Number of layers	Learning rate
#2	32	3	20	–	1	0.005
#3	64	3	50	–	1	0.01
#4	64	5	100	–	1	0.01
#5	32	5	100	–	1	0.01
#6	32	3	100	50	1	0.01

Fig. 11 shows the penetration rate from Changsha, where a full blue line represents measured values, and a dotted orange line represents predicted values. The univariate RNN model perfectly fits the next-step penetration rate in the training data. The trained model is evaluated using unseen data from Zhengzhou. The test results closely follow the trend of measured data with *RMSE* of 0.4034. The value of R^2 is equal to 0.6741, indicating a correlation between measured and predicted values in Fig. 12. It is worth noting that data points changing rapidly are hard to predict, and in comparison, the RNN algorithm proves to be more powerful than the statistical ARIMA method.

5.2. Multivariate models

5.2.1. Effects of input parameters

Apart from univariate models, multivariate models take into account the impact of other geological and operational parameters on TBM performance. Model #3 incorporates GEO, Model #4 incorporates OP, and Model #5 incorporates both GEO and OP. Model #3 and Model #4 are shown in Fig. 13a and b, in which good agreements between the measured and predicted values are shown. When geological parameters are added to the Model #3, the results are with *RMSE* of 0.4046 and R^2 of 0.6718. In contrast, Model #4 with operational parameters has a lower performance with *RMSE* of 0.4147 and R^2 of 0.6593. Model #5, in Fig. 13c, shows the measured penetration rate and the predicted values, resulting in *RMSE* of 0.4053 and R^2 of 0.6638.

However, the multivariate models do not perform much better than the univariate RNN model in Model #2. It is counter-intuitive that incorporating other parameters does not improve the accuracy of time series forecasting, probably due to the additional parameters increasing model complexity with both helpful and irrelevant information. This irrelevant information negatively affects feature extraction and degrades model performance.

5.2.2. RNN variants

Alternatively, the RNN variant reconfigures the inputs into two components: A time series of PR and the last-step GEO and OP. The time series of penetration rate PR_{t-2}, PR_{t-1}, PR_t are fed into RNN one by one, producing current hidden state h_t, as shown in Fig. 3. At the same time, the last-step geological and operational parameters GEO_t, OP_t are fully connected to extract hidden features $\overline{h}_t$. The output PR_{t+1} is then fully connected with h_t and $\overline{h}_t$ in a linear transformation.

Fig. 14 illustrates measured and predicted values by the RNN variant. Among these models, Model #6 has the lowest *RMSE* at 0.3952 and the highest R^2 at 0.6913. Therefore, the proposed method successfully improves the model performance because the

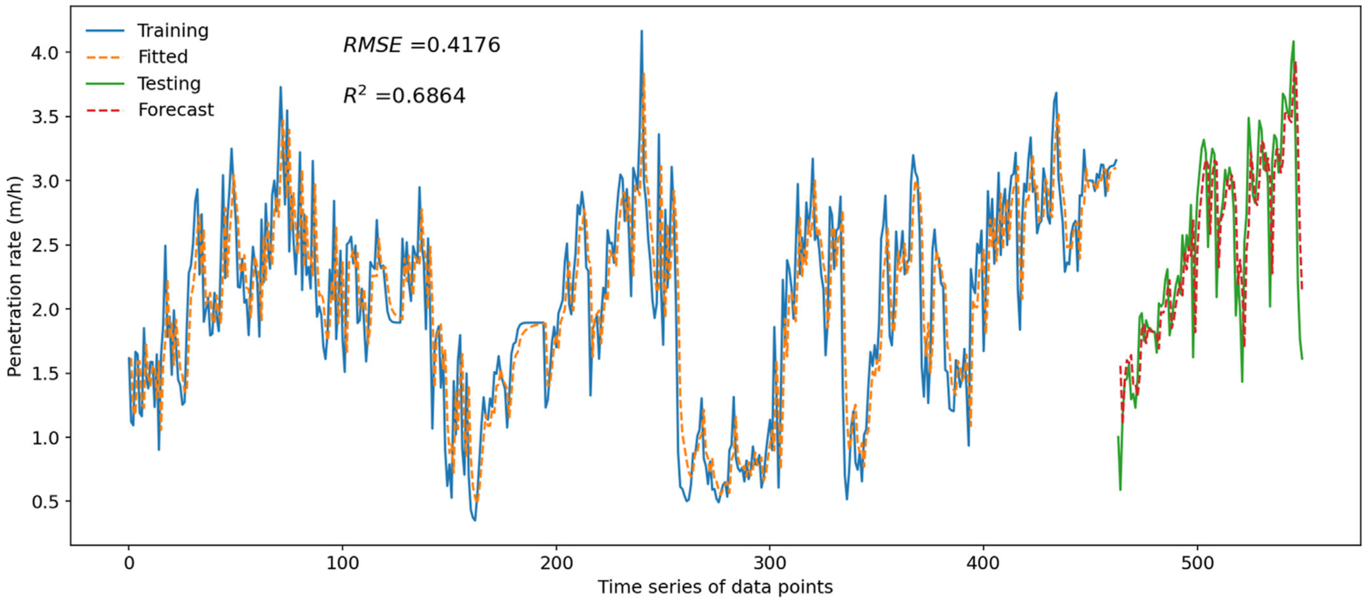

Fig. 9. Predicted and measured results in the one-step forecast by ARIMA in Model #1.

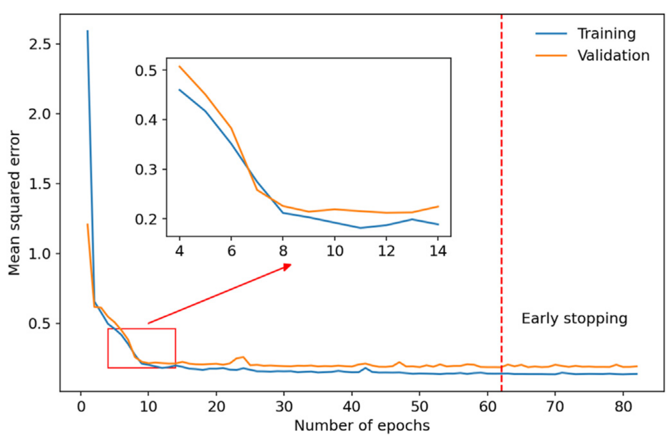

Fig. 10. Loss function of training and validation subsets against epochs.

last-step geological and operational parameters are closer to the future penetration rate.

5.3. Sensitivity analysis

Good generalisability is observed as the predicted values closely follow the trends of the measured values in both training and testing. Machine learning models are highly nonlinear, so the relationship between the input and output is usually poorly understood. The Sobol method is widely used to study the impacts of independent inputs on the output. For example, in Model #6, the input includes the last-three-step penetration rate and last-step geological and operational parameters. There are four steps in the method.

(1) Defining the range of parameters from 0 to 1 because all inputs are min-max normalised;
(2) Generating 1024 samples from the pseudo-random Sobol sequence to create 24,576 ($= 2 \times (11 + 1) \times 1024$) parameter sets in total;
(3) Running the parameter sets through Model #6 to calculate the output; and
(4) Sending the output back to calculate Sobol indices.

Fig. 15 displays the first-order Sobol index in Model #6. The time series of penetration rate is the most important parameter, with $S_{\{PR_t\}}$ of 0.8681, and the last-step penetration rate is the most important time, with S_{PR_t} of 0.7191. The range of the training data is usually expected to cover the test data. Nevertheless, the geological conditions between Changsha and Zhengzhou are quite different. According to the results of $S_{GEO_t} = 0.0429$ and $S_{OP_t} = 0.0861$, it is found that other geological and operational inputs in Model #6 have little effect on predicting penetration rate in the future.

5.4. Effects of data smoothing

Noise in a time series can obscure its intrinsic characteristics. After data smoothing by EMA, the kernel density estimations of residuals are in normal distributions with a mean of 0, as shown in Fig. 8b. However, the standard deviation of residuals increases as the smoothing factor decreases. Although a time series of noise is in a normal distribution, the normally distributed residuals are not necessarily noise. There is no clear distinction between noise and clean data, as both are vibrations in the sequence. A reasonable assumption is that normally distributed residuals represent different levels of noise, and the smoothed data remain clean data to varying extents.

Concerning the effects of data smoothing, additional models are conducted in time series forecasting. The original data ($\alpha = 1$) are processed by EMA with various smoothing factors ranging from 0.67 to 0.2. In Fig. 16, the correlation of determination R^2 between the original and smoothed data gradually decreases from 0.9456 to 0.8807, 0.7858, and 0.6718 with decreasing smoothing factor. Notably, the smoothing factor of 0.67 has the least smoothing effect, while a value of 0.2 results in the most significant smoothing effect.

We use RNN to predict next penetration rate, in order to exclude the effects of other parameters and focus solely on changes in the time series. Fig. 17 shows the results of Models #7–10 on evaluation metrics against varying smoothing factors, where the algorithm architecture and learning process are the same with that of Model

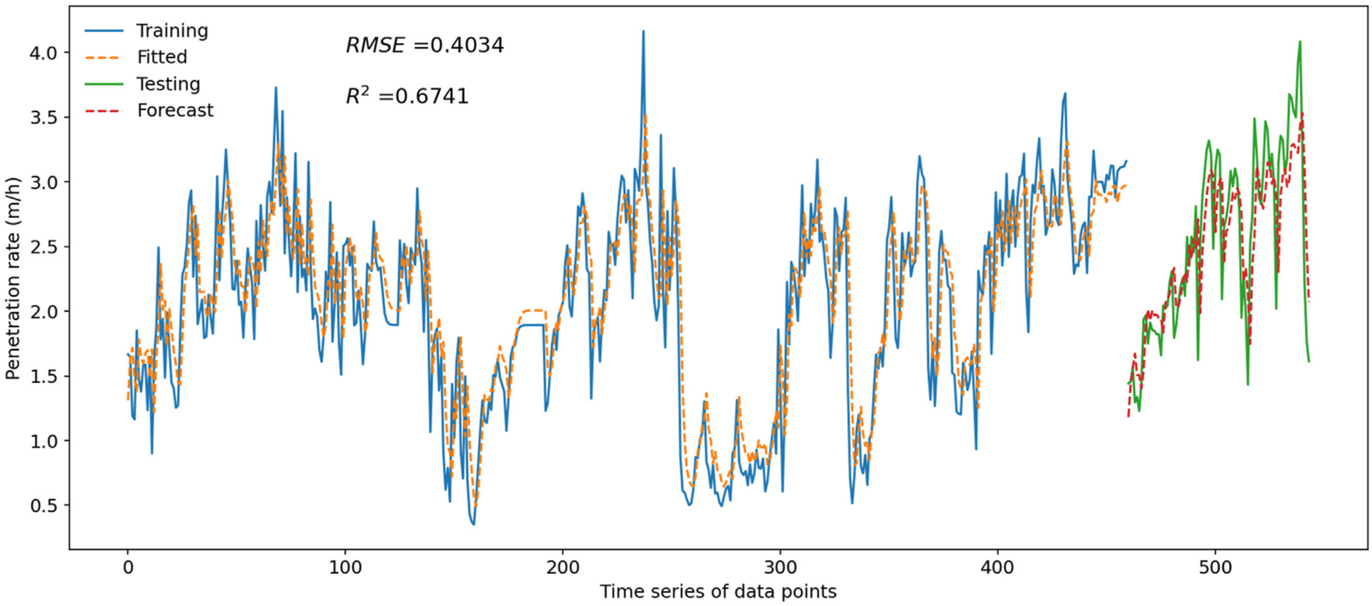

Fig. 11. Measured and predicted results in the one-step forecast by RNN in Model #2.

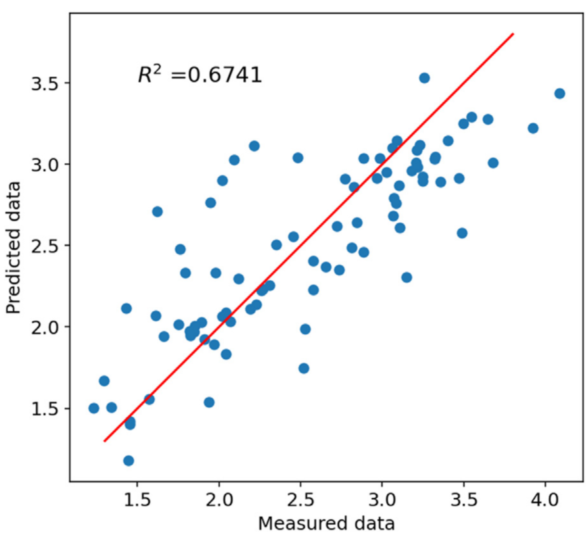

Fig. 12. R^2 between measured and predicted data.

#2. As the smoothing factor decreases, *RMSE* decreases from 0.6164 to 0.4034, 0.3092, 0.2026, and 0.1239. The value of R^2 is 0.4061 in original data and becomes 0.961 when $\alpha = 0.2$ in smoothed data.

On the one hand, the next-step penetration rate is easier to predict when the time series is smoother. For example, Model #10 ($\alpha = 0.2$) removes the largest extent of noise by EMA, resulting in the best model performance with *RMSE* of 0.1239 and R^2 of 0.961. On the other hand, over-simplified data can also eliminate underlying characteristics, raising a question about whether smoothed data can represent real characteristics of the data.

It is a dilemma that the original data can contain too much noise and be difficult in predicting the next-step penetration rate, while over-simplified data can lose important characteristics in the time series. In order to balance these factors, we conservatively choose a smoothing factor of 0.67 in the tests mentioned above. This allowed us to remove some of the noise while preserving the important features of the data as much as possible. In practical engineering, the residuals between original and smoothed data are sufficiently in a normal distribution, or wavelet transform assumes that noise is high-frequency components after sequential decomposition (Shi et al., 2021).

6. Limitation and further work

We have developed RNN variants that accurately predict penetration rate of the near future. Nevertheless, some limitations warrant further research.

(1) It is difficult to predict the future TBM performance of any meaningful time horizon using high-frequency data.
(2) Data smoothing can improve the forecast accuracy and increase the time horizon to the future, but risks over-smoothing that can lead to loss of data characteristics

The machine specifications, similar to cutterhead diameter and cutter arrangement, are neglected because they remain unchanged in the two tunnelling projects. We plan to continue this work when more reliable datasets become publicly available. It would be worthwhile to test other advanced algorithms, e.g. gated recurrent unit (Zhang et al., 2022b), WaveNet (Oord et al., 2016), DeepAR (Salinas et al., 2020) and Transformer (Vaswani et al., 2017), which have proven to be versatile and robust for time series problems. Because deep learning models are black boxes lacking interpretability, theory-guided machine learning (Karpatne et al., 2017) and physics-informed machine learning (Chen et al., 2021) are promising to provide physical meanings in time series forecasting.

7. Conclusions

This paper studies time series forecasting of TBM penetration rate, which is crucial for project time management, cost control, and risk mitigation. The modelling framework includes data processing, training and evaluation using various methods, e.g. ARIMA, RNN, and RNN variants.

Please cite this article as: Shan F et al., Effects of data smoothing and recurrent neural network (RNN) algorithms for real-time forecasting of tunnel boring machine (TBM) performance, Journal of Rock Mechanics and Geotechnical Engineering, https://doi.org/10.1016/j.jrmge.2023.06.015

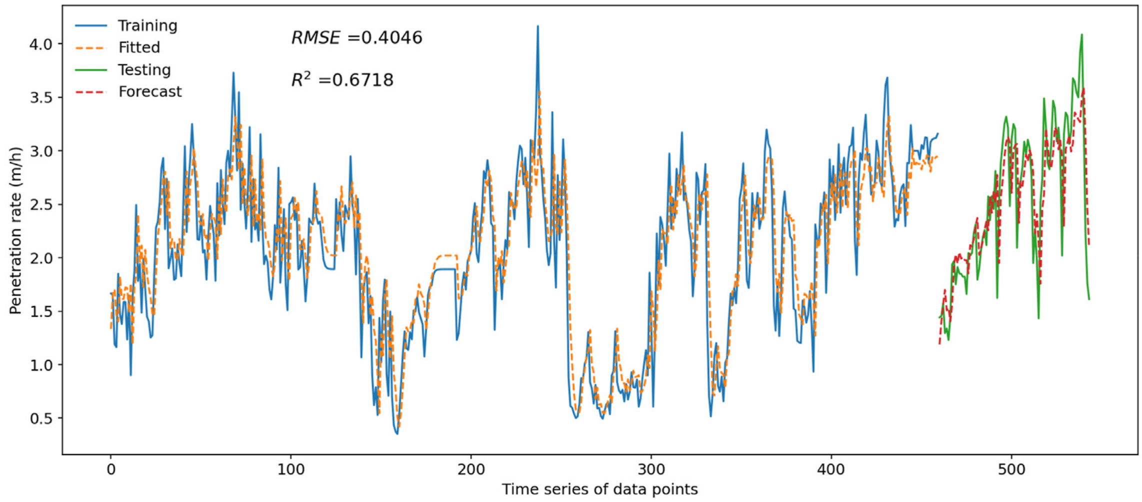

(a)

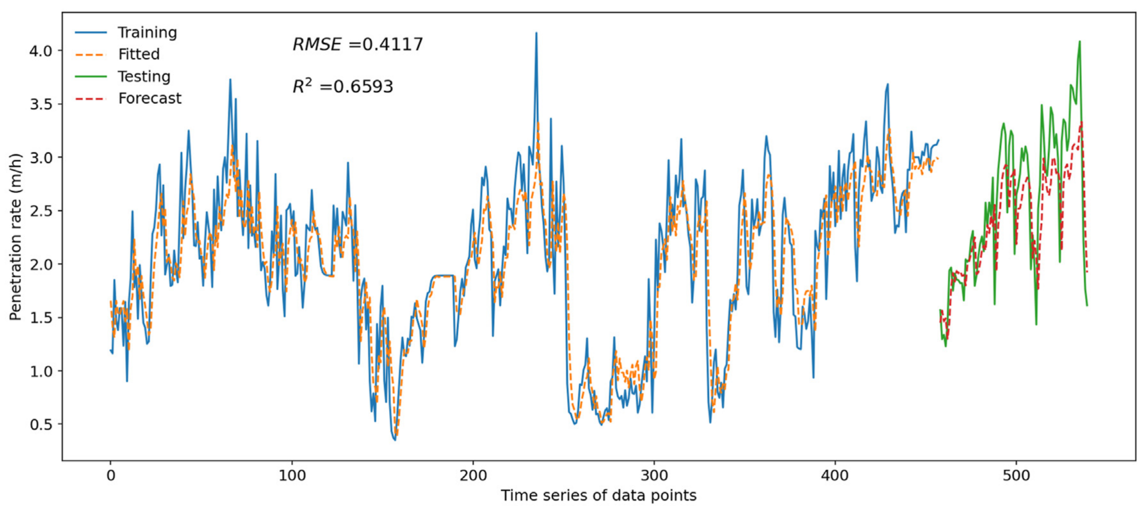

(b)

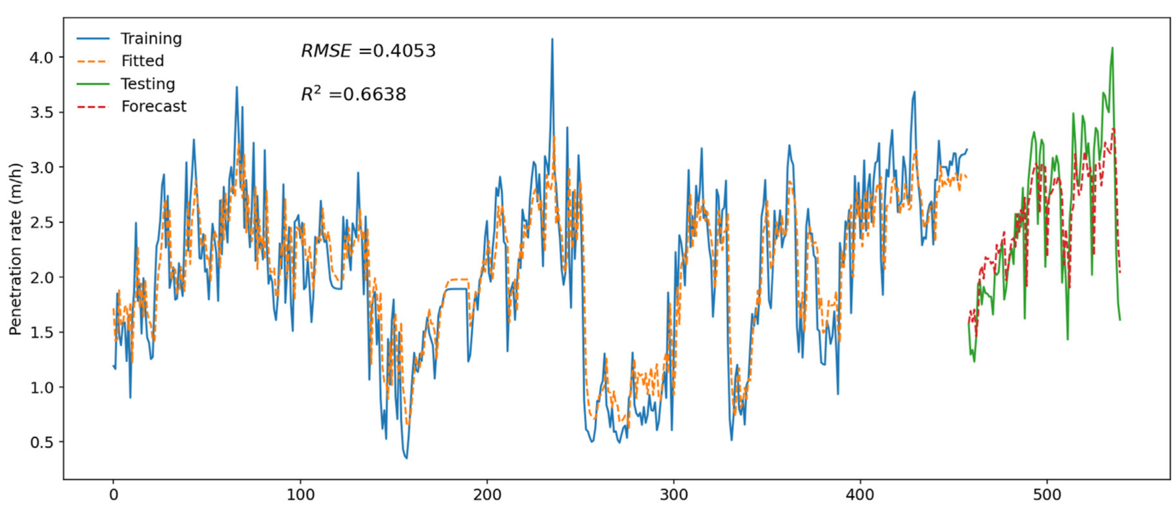

(c)

Fig. 13. Measured and predicted results in the one-step forecast by RNN in (a) Model #3, (b) Model #4, and (c) Model #5.

Please cite this article as: Shan F et al., Effects of data smoothing and recurrent neural network (RNN) algorithms for real-time forecasting of tunnel boring machine (TBM) performance, Journal of Rock Mechanics and Geotechnical Engineering, https://doi.org/10.1016/j.jrmge.2023.06.015

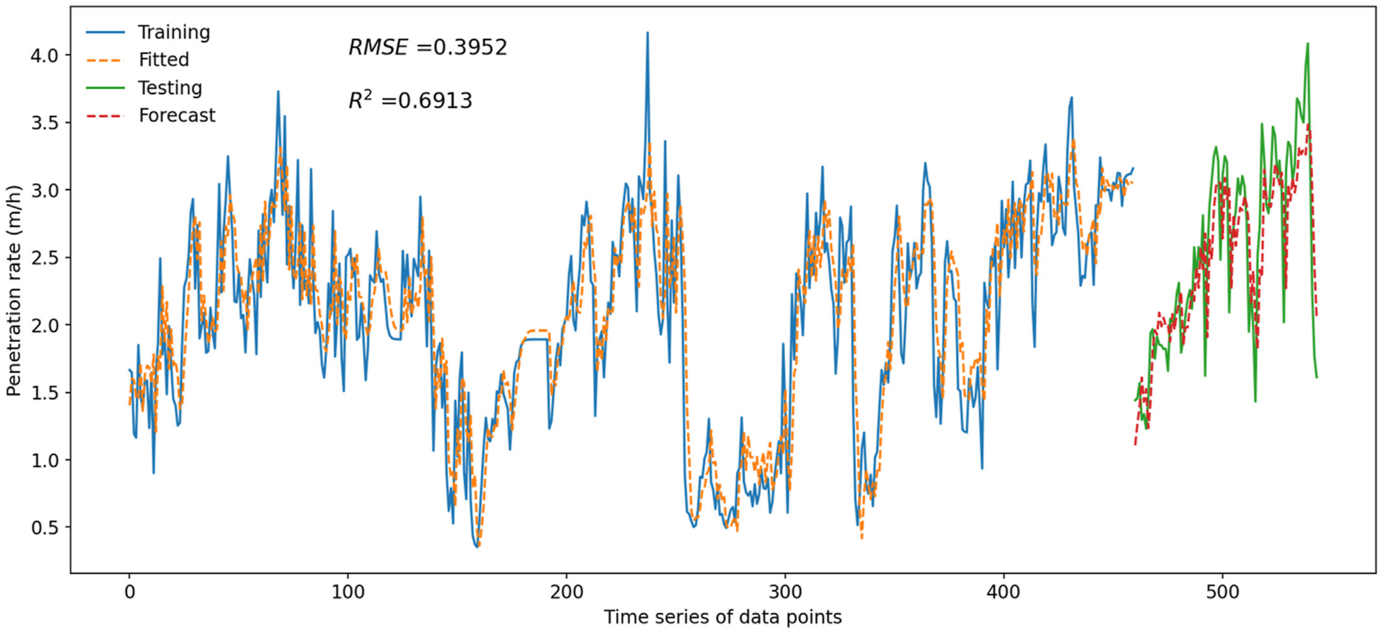

Fig. 14. Measured and predicted results in the one-step forecast by RNN variant in Model #6.

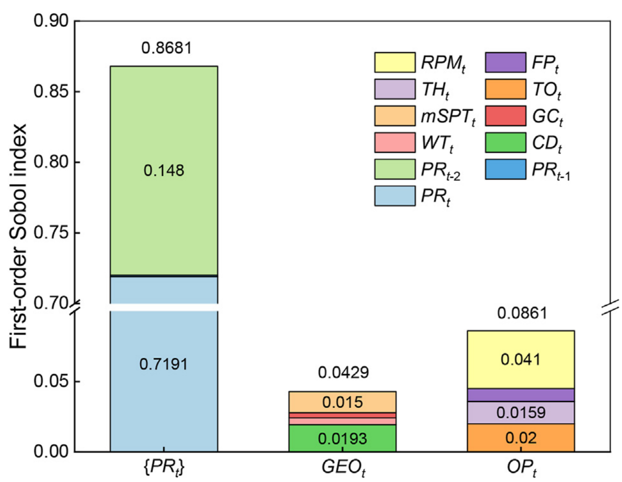

Fig. 15. First-order Sobol index for one-step forecasts in Model #6.

(1) In time series forecasting, univariate models are built for predicting the next-step penetration rate using ARIMA and RNN. Both models exhibit good performance in training and testing, with the RNN algorithm performing better than the statistical method of ARIMA. However, multivariate RNN models, incorporating the time series of geological and operational parameters, perform slightly worse than the univariate RNN model. This study develops an RNN variant that splits the inputs into a time series of penetration rate and last-step other parameters, which successfully improves model accuracy.

(2) Good generalisability is found even when the geological conditions in testing are different from those in training. According to the sensitivity analysis, time series of penetration rate is the most important parameter, while other parameters, including geological conditions, have little impact

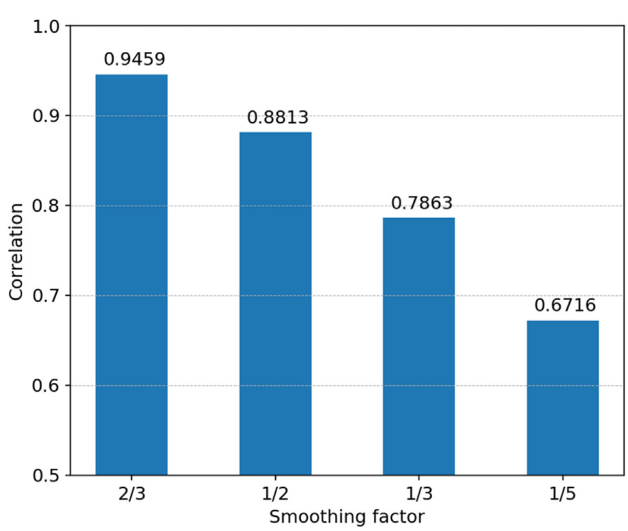

Fig. 16. Correlation between original and smoothed data of varying smoothing factors.

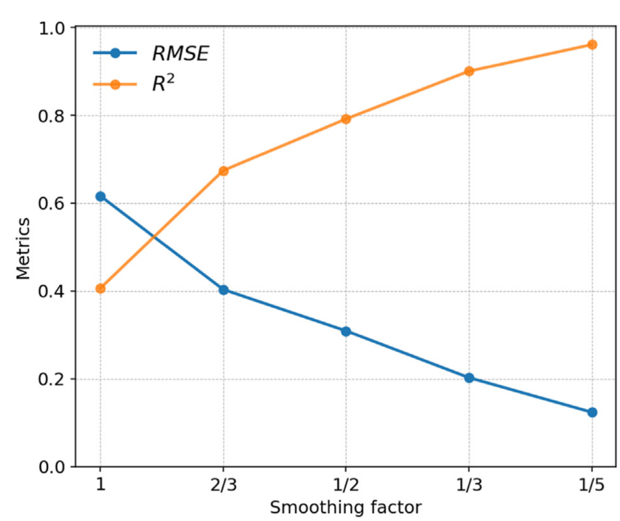

Fig. 17. Effects of data smoothing on one-step forecast evaluated by *RMSE* and R^2.

Please cite this article as: Shan F et al., Effects of data smoothing and recurrent neural network (RNN) algorithms for real-time forecasting of tunnel boring machine (TBM) performance, Journal of Rock Mechanics and Geotechnical Engineering, https://doi.org/10.1016/j.jrmge.2023.06.015

on the time series forecast. Geological conditions can become relevant if they do not vary much from training to test data.

(3) Data smoothing can effectively removes noise in the time series. It is found that smoothed data are easier to predict than original data. However, over-simplified data can lose real characteristics in the time series. It is a balance between noise reduction and real data preservation in time series forecasting.

Declaration of competing interest

The authors declare that they have no known competing financial interests or personal relationships that could have appeared to influence the work reported in this paper.

References

Armaghani, D.J., Mohamad, E.T., Narayanasamy, M.S., Narita, N., Yagiz, S., 2017. Development of hybrid intelligent models for predicting TBM penetration rate in hard rock condition. Tunn. Undergr. Space Technol. 63, 29–43.

Armaghani, D.J., Koopialipoor, M., Marto, A., Yagiz, S., 2019. Application of several optimization techniques for estimating TBM advance rate in granitic rocks. J. Rock Mech. Geotech. Eng. 11 (4), 779–789.

Bardhan, A., Kardani, N., Guharay, A., et al., 2021. Hybrid ensemble soft computing approach for predicting penetration rate of tunnel boring machine in a rock environment. J. Rock Mech. Geotech. Eng. 13 (6), 1398–1412.

Barton, N., 1999. TBM performance estimation in rock using Q(TBM). Tunn. Tunn. Int. 31 (9), 30–34.

Benardos, A., Kaliampakos, D., 2004. Modelling TBM performance with artificial neural networks. Tunn. Undergr. Space Technol. 19 (6), 597–605.

Bengio, Y., Simard, P., Frasconi, P., 1994. Learning long-term dependencies with gradient descent is difficult. IEEE Trans. Neural Network. 5 (2), 157–166.

Bontempi, G., Taieb, S.B., Le Borgne, Y.-A., 2012. Machine learning strategies for time series forecasting. In: European Business Intelligence Summer School, pp. 62–77. Springer.

Box, G.E., Pierce, D.A., 1970. Distribution of residual autocorrelations in autoregressive-integrated moving average time series models. J. Am. Stat. Assoc. 65 (332), 1509–1526.

Bruland, A., 1998. Hard Rock Tunnel Boring. Norwegian University of Science and Technology, Trondheim, Norway.

Chen, Z., Liu, Y., Sun, H., 2021. Physics-informed learning of governing equations from scarce data. Nat. Commun. 12 (1), 1–13.

Erharter, G.H., Marcher, T., 2021. On the pointlessness of machine learning based time delayed prediction of TBM operational data. Autom. Constr. 121, 103443.

Feng, S., Chen, Z., Luo, H., et al., 2021. Tunnel boring machines (TBM) performance prediction: a case study using big data and deep learning. Tunn. Undergr. Space Technol. 110, 103636.

Gao, X., Shi, M., Song, X., Zhang, C., Zhang, H., 2019. Recurrent neural networks for real-time prediction of TBM operating parameters. Autom. Constr. 98, 225–235.

Graves, A., Mohamed, A.-R., Hinton, G., 2013. Speech recognition with deep recurrent neural networks. In: Proceedings of the 2013 IEEE International Conference on Acoustics, Speech and Signal Processing, pp. 6645–6649. IEEE.

Grima, M.A., Bruines, P., Verhoef, P., 2000. Modeling tunnel boring machine performance by neuro-fuzzy methods. Tunn. Undergr. Space Technol. 15 (3), 259–269.

Hassanpour, J., Rostami, J., Khamehchiyan, M., Bruland, A., Tavakoli, H., 2010. TBM performance analysis in pyroclastic rocks: a case history of Karaj water conveyance tunnel. Rock Mech. Rock Eng. 43 (4), 427–445.

Hasanpour, R., Rostami, J., Schmitt, J., Ozcelik, Y., Sohrabian, B., 2020. Prediction of TBM jamming risk in squeezing grounds using Bayesian and artificial neural networks. J. Rock Mech. Geotech. Eng. 12 (1), 21–31.

Hoeffding, W., 1992. A class of statistics with asymptotically normal distribution. In: Breakthroughs in Statistics, pp. 308–334. Springer.

Hou, S., Liu, Y., Yang, Q., 2022. Real-time prediction of rock mass classification based on TBM operation big data and stacking technique of ensemble learning. J. Rock Mech. Geotech. Eng. 14 (1), 123–143.

Huang, X., Zhang, Q., Liu, Q., et al., 2022. A real-time prediction method for tunnel boring machine cutter-head torque using bidirectional long short-term memory networks optimized by multi-algorithm. J. Rock Mech. Geotech. Eng. 14 (3), 798–812.

Kannangara, K.P.M., Zhou, W., Ding, Z., Hong, Z., 2022. Investigation of feature contribution to shield tunneling-induced settlement using Shapley additive explanations method. J. Rock Mech. Geotech. Eng. 14 (4), 1052–1063.

Karpatne, A., Atluri, G., Faghmous, J.H., et al., 2017. Theory-guided data science: a new paradigm for scientific discovery from data. IEEE Trans. Knowl. Data Eng. 29 (10), 2318–2331.

Li, J., Li, P., Guo, D., Li, X., Chen, Z., 2021. Advanced prediction of tunnel boring machine performance based on big data. Geosci. Front. 12 (1), 331–338.

Lin, S., Shen, S., Zhang, N., Zhou, A., 2021. Modelling the performance of EPB shield tunnelling using machine and deep learning algorithms. Geosci. Front. 12 (5), 101177.

Lin, S., Zhang, N., Zhou, A., Shen, S., 2022a. Time-series prediction of shield movement performance during tunneling based on hybrid model. Tunn. Undergr. Space Technol. 119, 104245.

Lin, S., Shen, S., Zhou, A., 2022b. Real-time analysis and prediction of shield cutterhead torque using optimized gated recurrent unit neural network. J. Rock Mech. Geotech. Eng. 14 (4), 1232–1240.

Liu, M., Liao, S., Yang, Y., et al., 2021. Tunnel boring machine vibration-based deep learning for the ground identification of working faces. J. Rock Mech. Geotech. Eng. 13 (6), 1340–1357.

Mahdevari, S., Shahriar, K., Yagiz, S., Shirazi, M.A., 2014. A support vector regression model for predicting tunnel boring machine penetration rates. Int. J. Rock Mech. Min. Sci. 72, 214–229.

Oord, A.V.D., Dieleman, S., Zen, H., et al., 2016. Wavenet: A Generative Model for Raw Audio arXiv:1609.03499.

Ozdemir, L., 1977. Development of Theoretical Equations for Predicting Tunnel Boreability. Colorado School of Mines.

Parsajoo, M., Mohammed, A.S., Yagiz, S., Armaghani, D.J., Khandelwal, M., 2021. An evolutionary adaptive neuro-fuzzy inference system for estimating field penetration index of tunnel boring machine in rock mass. J. Rock Mech. Geotech. Eng. 13 (6), 1290–1299.

Pavlyshenko, B.M., 2019. Machine-learning models for sales time series forecasting. Data 4 (1), 15.

Qin, C., Shi, G., Tao, J., et al., 2021. Precise cutterhead torque prediction for shield tunneling machines using a novel hybrid deep neural network. Mech. Syst. Signal Process. 151, 107386.

Roberts, S., 2000. Control chart tests based on geometric moving averages. Technometrics 42 (1), 97–101.

Rostami, J., Ozdemir, L., Nilson, B., 1996. Comparison between CSM and NTH hard rock TBM performance prediction models. In: Proceedings of Annual Technical Meeting of the Institute of Shaft Drilling Technology, pp. 1–10. Las Vegas.

Rostami, J., 1997. Development of a Force Estimation Model for Rock Fragmentation with Disc Cutters through Theoretical Modeling and Physical Measurement of Crushed Zone Pressure. PhD Thesis. Colorado School of Mines, Golden, CO, USA.

Rostami, J., 2016. Performance prediction of hard rock Tunnel Boring Machines (TBMs) in difficult ground. Tunn. Undergr. Space Technol. 57, 173–182.

Salimi, A., Rostami, J., Moormann, C., Delisio, A., 2016. Application of non-linear regression analysis and artificial intelligence algorithms for performance prediction of hard rock TBMs. Tunn. Undergr. Space Technol. 58, 236–246.

Salinas, D., Flunkert, V., Gasthaus, J., Januschowski, T., 2020. DeepAR: Probabilistic forecasting with autoregressive recurrent networks. Int. J. Forecast. 36 (3), 1181–1191.

Sapigni, M., Berti, M., Bethaz, E., Busillo, A., Cardone, G., 2002. TBM performance estimation using rock mass classifications. Int. J. Rock Mech. Min. Sci. 39 (6), 771–788.

Schuster, M., Paliwal, K.K., 1997. Bidirectional recurrent neural networks. IEEE Trans. Signal Process. 45 (11), 2673–2681.

Shan, F., He, X., Armaghani, D.J., Zhang, P., Sheng, D., 2022. Success and challenges in predicting TBM penetration rate using recurrent neural networks. Tunn. Undergr. Space Technol. 130, 104728.

Shan, F., He, X., Armaghani, D.J., Zhang, P., Sheng, D., 2023. Response to Discussion on "Success and challenges in predicting TBM penetration rate using recurrent neural networks" by Georg H. Erharter, Thomas Marcher. Tunn. Undergr. Space Technol. 139, 105064.

Shi, G., Qin, C., Tao, J., Liu, C., 2021. A VMD-EWT-LSTM-based multi-step prediction approach for shield tunneling machine cutterhead torque. Knowl. Based Syst. 228, 107213.

Sobol, I.M., 1990. On sensitivity estimation for nonlinear mathematical models. Matematicheskoe Modelirovanie 2 (1), 112–118.

Sousa, R.L., Einstein, H.H., 2012. Risk analysis during tunnel construction using Bayesian Networks: porto Metro case study. Tunn. Undergr. Space Technol. 27 (1), 86–100.

Sun, W., Shi, M., Zhang, C., Zhao, J., Song, X., 2018. Dynamic load prediction of tunnel boring machine (TBM) based on heterogeneous in-situ data. Autom. Constr. 92, 23–34.

Vaswani, A., Shazeer, N., Parmar, N., et al., 2017. Attention is all you need. In: Proceedings of the 31st Conference on Neural Information Processing Systems (NIPS 2017). Long Beach, CA, USA.

Wang, R., Li, D., Chen, E.J., Liu, Y., 2021. Dynamic prediction of mechanized shield tunneling performance. Autom. Constr. 132, 103958.

Wu, Z., Wei, R., Chu, Z., Liu, Q., 2021. Real-time rock mass condition prediction with TBM tunneling big data using a novel rock–machine mutual feedback perception method. J. Rock Mech. Geotech. Eng. 13 (6), 1311–1325.

Xu, C., Liu, X., Wang, E., Wang, S., 2021. Prediction of tunnel boring machine operating parameters using various machine learning algorithms. Tunn. Undergr. Space Technol. 109, 103699.

Yagiz, S., 2002. PhD Thesis. In: Development of Rock Fracture and Brittleness Indices to Quantify the Effects of Rock Mass Features and Toughness in the CSM Model Basic Penetration for Hard Rock Tunneling Machines. Colorado School of Mines, Golden, CO, USA.

Yagiz, S., 2008. Utilizing rock mass properties for predicting TBM performance in hard rock condition. Tunn. Undergr. Space Technol. 23 (3), 326–339.

Please cite this article as: Shan F et al., Effects of data smoothing and recurrent neural network (RNN) algorithms for real-time forecasting of tunnel boring machine (TBM) performance, Journal of Rock Mechanics and Geotechnical Engineering, https://doi.org/10.1016/j.jrmge.2023.06.015

Yagiz, S., Karahan, H., 2011. Prediction of hard rock TBM penetration rate using particle swarm optimization. Int. J. Rock Mech. Min. Sci. 48 (3), 427–433.
Yagiz, S., Karahan, H., 2015. Application of various optimization techniques and comparison of their performances for predicting TBM penetration rate in rock mass. Int. J. Rock Mech. Min. Sci. 80, 308–315.
Yang, H., Wang, Z., Song, K., 2022. A new hybrid grey wolf optimizer-feature weighted-multiple kernel-support vector regression technique to predict TBM performance. Eng. Comput. 38 (4), 2469–2485.
Zhang, P., Chen, R., Wu, H., 2019. Real-time analysis and regulation of EPB shield steering using Random Forest. Autom. Constr. 106, 102860.
Zhang, P., Wu, H., Chen, R., et al., 2020a. A critical evaluation of machine learning and deep learning in shield-ground interaction prediction. Tunn. Undergr. Space Technol. 106, 103593.
Zhang, Q., Hu, W., Liu, Z., Tan, J., 2020b. TBM performance prediction with Bayesian optimization and automated machine learning. Tunn. Undergr. Space Technol. 103, 103493.
Zhang, W., Li, H., Wu, C., et al., 2021a. Soft computing approach for prediction of surface settlement induced by earth pressure balance shield tunneling. Undergr. Space 6 (4), 353–363.
Zhang, W., Li, H., Li, Y., et al., 2021b. Application of deep learning algorithms in geotechnical engineering: a short critical review. Artif. Intell. Rev. 54, 5633–5673.
Zhang, P., Chen, R., Dai, T., Wang, Z., Wu, K., 2021c. An AIoT-based system for real-time monitoring of tunnel construction. Tunn. Undergr. Space Technol. 109, 103766.
Zhang, W., Wu, C., Zhong, H., Li, Y., Wang, L., 2021d. Prediction of undrained shear strength using extreme gradient boosting and random forest based on Bayesian optimization. Geosci. Front. 12 (1), 469–477.
Zhang, W., Wu, C., Tang, L., Gu, X., Wang, L., 2022a. Efficient time-variant reliability analysis of bazimen landslide in the three gorges reservoir area using XGBoost and LightGBM algorithms. Gondwana Res. https://doi.org/10.1016/j.gr.2022.10.004.
Zhang, W., Li, H., Tang, L., et al., 2022b. Displacement prediction of Jiuxianping landslide using gated recurrent unit (GRU) networks. Acta Geotech 17 (4), 1367–1382.

Feng Shan obtained his BSc and MSc degrees in civil engineering from China University of Geosciences (Wuhan) and Central South University, China, in 2016 and 2019, respectively. He is currently a PhD candidate in civil engineering at the University of Technology Sydney, Australia. His research interests lie in the innovative intersection of numerical modelling in unsaturated soils, intelligent TBM tunnelling, and machine learning. He has published six journal articles and two conference papers.

Please cite this article as: Shan F et al., Effects of data smoothing and recurrent neural network (RNN) algorithms for real-time forecasting of tunnel boring machine (TBM) performance, Journal of Rock Mechanics and Geotechnical Engineering, https://doi.org/10.1016/j.jrmge.2023.06.015